Fourth Workshop on
Physics and Computation
Boston University, 22–24 Nov. 1996.

In: T. Toffoli, M. Biafore, and J. Leão (ed.), *PhysComp96*, New England Complex Systems Institute (1996), 87–91.
Also on-line in the *InterJournal*.

submitted: 12 May 1996
revised: 25 Oct., 17 Nov. 1996

Nuclear magnetic resonance spectroscopy: an experimentally accessible paradigm for quantum computing*

David G. Cory†
Nuclear Eng. Dept., M.I.T.
Amr F. Fahmy‡
Div. of Applied Sciences, Harvard University
Timothy F. Havel‡
B.C.M.P., Harvard Medical School

1 Introduction

The theory of quantum computing is advancing at a rate which vastly outstrips its experimental realization (for recent accounts, see [1, 2, 3]). Most attempts to implement a quantum computer have utilized submicroscopic assemblies of quantum spins, which are difficult to prepare, isolate, manipulate and observe. A "homologous" system which exhibits many of the same properties, but is easier to work with, would clearly be very useful both as a means of testing theoretical predictions, and for demonstration and educational purposes. Such a system is provided by weakly polarized macroscopic ensembles of spins, which are readily manipulated and observed by *nuclear magnetic resonance spectroscopy*, or NMR.

The spins of a molecule in solution are largely isolated from their surroundings by simple surface to volume considerations, and from spins in neighboring molecules by rotational averaging, which reduces dipole-dipole coupling to a second-order effect[4]. This fact enables us to work with a *reduced density matrix* $\mathbf{D}$ of size 2^n, where n is the number of spin 1/2 nuclei in the molecule, rather than 2^N where N is the total number of such spins in the sample[5]. It is also customary in NMR spectroscopy to shift the reduced density matrix by subtraction of 2^{-n} times the trace of the equilibrium reduced density matrix, since only the traceless part undergoes unitary evolution, and to scale it to have integral elements[6]. In the next paragraph, we define a manifold of statistical spin states with a reduced density matrix whose traceless part is proportional to the traceless part of the usual density matrix of a pure state.

In the following, whenever we use the term "density matrix", we mean "reduced, shifted and scaled density matrix" unless otherwise stated. When such a density matrix has rank equal to one (after adding an appropriate multiple of the unit matrix to it), it can be factored into a dyadic product of the coordinates of a "spinor" and its conjugate versus the usual $\mathbf{I}_z$ basis, and this factorization is unique up to an overall phase factor. This mapping between spinor coordinates and density matrices which can be shifted to a signature of $[1, 0, \dots, 0]$ is *covariant*, in the sense that if we apply a unitary matrix to a spinor's coordinates, the corresponding density matrix transforms by conjugation with the *same* unitary matrix. As a result, we can regard such a density matrix as a kind of spinor, and perform essentially arbitrary unitary transformations on it via NMR spectroscopy, thereby "emulating" a quantum computer. We shall call the states described by density matrices with one positive and $2^n - 1$ equal negative eigenvalues "pseudo-pure" states, and the corresponding spinors "pseudo-spinors".

Of course, some things are lost in translation. For example, the density matrix is not changed on rotation by 2π, although spinors change sign. Since these sign changes cannot easily be observed, this seems to be of little consequence for quantum computing. More important is the fact that the coherence which is observed by NMR spectroscopy is always an ensemble average over an astronomical number of microscopic systems. As a consequence, the NMR spectrum of a pseudo-pure state yields the expectation values of certain observables relative to the corresponding pseudo-spinor, rather than a random eigenvalue of one of them. In particular, *wave function collapse does not occur*. A wide variety of more easily controlled "filtering" mechanisms are available in NMR spectroscopy, however, and we have shown that for most computational purposes the ability to measure expectation values directly is actually a great advantage[8]. NMR experiments on liquid samples possess a number of other highly desirable features as well; in particular, the decoherence times are typically on the order of seconds.

We claim that NMR spectroscopy in fact provides a means of building a nonconventional computer that can be programmed much like a quantum computer, and is capable of the same exponential speed-ups, but is much easier to implement. In some respects, this approach also resembles DNA computing, in that it can use the parallelism inherent in ensembles of molecules to efficiently count the number of solutions to combinatorial problems. A detailed account of the theory may be found in [8]; this paper will describe how basic quantum logic gates can be implemented via NMR spectroscopy, and present experimental results to validate our claims. After submitting the revised version of this abstract, we learned that an analogous approach has also been submitted to this workshop[7].

*Correspondence should be directed to `havel@menelaus.med.harvard.edu`.
†Thanks NSF/DMR 9357603.
‡Thanks NSF/MCB 9527181.

2 Basic results from NMR

Let us begin with the simplest nontrivial case, namely a molecule in solution containing exactly two coupled spins. The dipolar coupling averages to zero in solution, but the so-called *scalar* coupling remains, which is mediated by electron correlation in the chemical bonds linking the atoms. It will simplify our presentation if we assume *weak coupling*, i.e. that the coupling constant J is small compared to the difference $|\omega_1 - \omega_2|$ in the resonance frequencies of the two spins. With the convention that the magnetic field is along the z-axis, the Hamiltonian of this system is $\mathbf{H} = \omega_1 \mathbf{I}_z^1 + \omega_2 \mathbf{I}_z^2 + 2\pi J\, \mathbf{I}_z^1 \mathbf{I}_z^2$, where $\mathbf{I}_z^k$ $(k = 1, 2)$ are the usual matrices for the z-component of the angular momentum of each spin. Because the energy level differences are small compared to kT at room temperature, the equilibrium density matrix of this system is given to an excellent approximation by $\mathbf{Exp}(-\mathbf{H}/kT) \approx \mathbf{1} - \mathbf{H}/kT$. On taking account of the fact that $J \ll \omega_1 \approx \omega_2$, removing the trace and scaling, the equilibrium density matrix becomes

$$\mathbf{D}_{eq} = \mathbf{I}_z^1 + \mathbf{I}_z^2 = \begin{pmatrix} 1 & 0 & 0 & 0 \\ 0 & 0 & 0 & 0 \\ 0 & 0 & 0 & 0 \\ 0 & 0 & 0 & -1 \end{pmatrix} . \qquad (1)$$

Rather than writing them out explicitly, NMR spectroscopists typically represent their density matrices as linear combinations of "product operators", i.e. the products of the usual matrices of one-spin operators $\mathbf{I}_x$, $\mathbf{I}_y$ and $\mathbf{I}_z$ (as above). This makes it very easy to describe the unitary transformations effected by applying RF (radio-frequency) pulses to the sample. For example, a $\pi/2$ pulse about the y-axis (in the rotating frame[6]) by definition rotates the equilibrium density matrix to

$$\mathbf{D}_{eq} \xrightarrow{[\pi/2]_y} \mathbf{I}_x^1 + \mathbf{I}_x^2 . \qquad (2)$$

This rotated magnetization precesses about the applied field and generates an oscillatory magnetic moment in the xy-plane, according to the density matrix obtained from the time-dependent unitary transformation:

$$\mathbf{Exp}(-it\mathbf{H})(\mathbf{I}_x^1 + \mathbf{I}_x^2)\mathbf{Exp}(it\mathbf{H}) \qquad (3)$$

The complex-valued, time-dependent signal that is detected is calculated by taking the trace of the product of this density matrix with

$$\mathbf{I}_+^1 + \mathbf{I}_+^2 = \begin{pmatrix} 0 & 1 & 1 & 0 \\ 0 & 0 & 0 & 1 \\ 0 & 0 & 0 & 1 \\ 0 & 0 & 0 & 0 \end{pmatrix} , \qquad (4)$$

where $\mathbf{I}_+ = \mathbf{I}_x + i\, \mathbf{I}_y$ as usual (see e.g. [4]). Since this matrix contains only four nonzero elements, the spectrum contains direct information on only four of the ten independent elements of the density matrix, namely $D_{12} = D_{21}^*, D_{13} = D_{31}^*, D_{24} = D_{42}^*$ and $D_{34} = D_{43}^*$. These elements are called *single-quantum coherences*. After Fourier transformation,

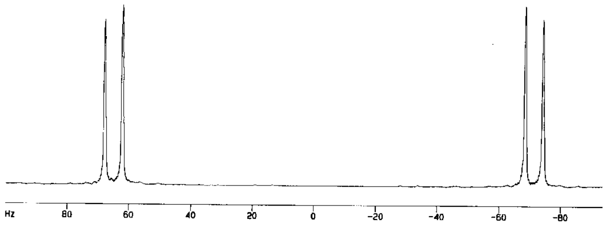

Figure 1: The experimental NMR spectrum of liquid 2,3-dibromo-thiophene (a molecule with two nonequivalent, weakly coupled spin 1/2 hydrogen atoms) after applying a nonselective $\pi/2$ y-pulse to the equilibrium state and Fourier transforming the resulting signal (see text).

we obtain a spectrum containing a pair of doublets as in Fig. 1.

If the *chemical shifts* (i.e. resonance frequencies relative to some standard) of the two spins differ by several times the sum of their line widths and coupling constant, such a pulse can be made selective for only one of the two spins, e.g. the second, which yields

$$\mathbf{D}_{eq} \xrightarrow{[\pi/2]_y^2} \mathbf{I}_z^1 + \mathbf{I}_x^2 . \qquad (5)$$

A *gradient pulse*, which produces a transient field inhomogeneity along the z-axis, can then be used to selectively quench the x-coherence, giving

$$\mathbf{I}_z^1 = \begin{pmatrix} 1/2 & 0 & 0 & 0 \\ 0 & 1/2 & 0 & 0 \\ 0 & 0 & -1/2 & 0 \\ 0 & 0 & 0 & -1/2 \end{pmatrix} . \qquad (6)$$

In a similar manner, we can generate the state

$$\mathbf{I}_z^2 = \begin{pmatrix} 1/2 & 0 & 0 & 0 \\ 0 & -1/2 & 0 & 0 \\ 0 & 0 & 1/2 & 0 \\ 0 & 0 & 0 & -1/2 \end{pmatrix} . \qquad (7)$$

A further $\pi/2$ pulse will convert this to $\mathbf{I}_x^2$, which evolves under the influence of a coupling constant of J Hz. to

$$\mathbf{I}_x^2 \cos(\pi J t) + 2\mathbf{I}_z^1 \mathbf{I}_y^2 \sin(\pi J t) . \qquad (8)$$

Thus after a period of $t = 1/(2J)$, we obtain $2\mathbf{I}_z^1 \mathbf{I}_y^2$. A final selective $\pi/2$ pulse can then be used to obtain the correlated state

$$2\mathbf{I}_z^1 \mathbf{I}_z^2 = \begin{pmatrix} 1/2 & 0 & 0 & 0 \\ 0 & -1/2 & 0 & 0 \\ 0 & 0 & -1/2 & 0 \\ 0 & 0 & 0 & 1/2 \end{pmatrix} . \qquad (9)$$

3 Pseudo-spinors in NMR

It is possible to generate all three of the states (6), (7) and (9) simultaneously in the same sample, yielding:

$$\mathbf{I}_z^1 + \mathbf{I}_z^2 + 2\mathbf{I}_z^1 \mathbf{I}_z^2 = \begin{pmatrix} 3/2 & 0 & 0 & 0 \\ 0 & -1/2 & 0 & 0 \\ 0 & 0 & -1/2 & 0 \\ 0 & 0 & 0 & -1/2 \end{pmatrix} \qquad (10)$$

This matrix shifts to

$$\begin{pmatrix} 2 & 0 & 0 & 0 \\ 0 & 0 & 0 & 0 \\ 0 & 0 & 0 & 0 \\ 0 & 0 & 0 & 0 \end{pmatrix} , \tag{11}$$

which can in turn be factorized into the product of a pseudo-spinor with its conjugate

$$2\,|00\rangle\langle 00| \;\equiv\; 2 \begin{pmatrix} 1 \\ 0 \\ 0 \\ 0 \end{pmatrix} \begin{pmatrix} 1 & 0 & 0 & 0 \end{pmatrix} . \tag{12}$$

Therefore, the matrix $\mathbf{I}_z^1 + \mathbf{I}_z^2 + 2\mathbf{I}_z^1\mathbf{I}_z^2$ in Eq. (10) represents a pseudo-pure state in product operator notation.

The following RF and gradient pulse sequence accomplishes this task:

$$\begin{array}{l} \mathbf{I}_z^1 + \mathbf{I}_z^2 \\ \xrightarrow{[\pi/3]_x^2} \mathbf{I}_z^1 + \mathbf{I}_z^2/2 - \mathbf{I}_y^2\sqrt{3}/2 \\ \xrightarrow{[z-\mathrm{grad}]} \mathbf{I}_z^1 + \mathbf{I}_z^2/2 \\ \xrightarrow{[\pi/4]_x^1} \mathbf{I}_z^1/\sqrt{2} + \mathbf{I}_z^2/2 - \mathbf{I}_y^1/\sqrt{2} \\ \xrightarrow{[1/(2J)]} \mathbf{I}_z^1/\sqrt{2} + \mathbf{I}_z^2/2 + \sqrt{2}\mathbf{I}_x^1\mathbf{I}_z^2 \\ \xrightarrow{[-\pi/4]_y^1} \mathbf{I}_z^1/2 + \mathbf{I}_z^2/2 - \mathbf{I}_x^1/2 - \mathbf{I}_x^1\mathbf{I}_z^2 + \mathbf{I}_z^1\mathbf{I}_z^2 \\ \xrightarrow{[z-\mathrm{grad}]} \mathbf{I}_z^1/2 + \mathbf{I}_z^2/2 + \mathbf{I}_z^1\mathbf{I}_z^2 \end{array} \tag{13}$$

This same pseudo-pure state can also be obtained by a variety of other methods. Indeed, all four *basic* pseudo-pure states (with density matrices shifting to a single positive element on the diagonal and zeros elsewhere) can be obtained. In terms of product operators, these can be written as:

$$\begin{array}{rcl} 2\,|00\rangle\langle 00| - \frac{1}{2}\mathbf{1} & \equiv & \mathbf{I}_z^1 + \mathbf{I}_z^2 + 2\mathbf{I}_z^1\mathbf{I}_z^2 \\ 2\,|01\rangle\langle 01| - \frac{1}{2}\mathbf{1} & \equiv & \mathbf{I}_z^1 - \mathbf{I}_z^2 - 2\mathbf{I}_z^1\mathbf{I}_z^2 \\ 2\,|10\rangle\langle 10| - \frac{1}{2}\mathbf{1} & \equiv & -\mathbf{I}_z^1 + \mathbf{I}_z^2 - 2\mathbf{I}_z^1\mathbf{I}_z^2 \\ 2\,|11\rangle\langle 11| - \frac{1}{2}\mathbf{1} & \equiv & -\mathbf{I}_z^1 - \mathbf{I}_z^2 + 2\mathbf{I}_z^1\mathbf{I}_z^2 \end{array} \tag{14}$$

Given a basic pseudo-pure state, a "coherent superposition" of pseudo-spinors can be prepared by a simple nonselective $\pi/2$ pulse, for example:

$$|00\rangle\langle 00| \xrightarrow{[\pi/2]_y} \frac{1}{4} \begin{pmatrix} 1 & 1 & 1 & 1 \\ 1 & 1 & 1 & 1 \\ 1 & 1 & 1 & 1 \\ 1 & 1 & 1 & 1 \end{pmatrix} \tag{15}$$

This matrix in turn is proportional to the dyadic product of the pseudo-spinor

$$\begin{array}{l} |00\rangle + |01\rangle + |10\rangle + |11\rangle \\ = (|0\rangle + |1\rangle)(|0\rangle + |1\rangle) \end{array} \tag{16}$$

with its conjugate. Since this can be further factorized into a product of one-spin pseudo-spinors (as shown), it represents an "unentangled" state.

An entangled state can be generated with a standard pulse sequence consisting of nonselective $\pi/2$ y-pulse followed by a delay of $1/(2J)$ and a second $\pi/2$ y-pulse*, i.e.

$$|00\rangle\langle 00| \xrightarrow{[\pi/2]_y - [1/(2J)] - [\pi/2]_y} \begin{pmatrix} 1/2 & 0 & 0 & -i/2 \\ 0 & 0 & 0 & 0 \\ 0 & 0 & 0 & 0 \\ i/2 & 0 & 0 & 1/2 \end{pmatrix} \tag{17}$$

In NMR circles, the nonzero off-diagonal locations in this matrix are referred to as a *double-quantum coherence*, since they correspond to a two-spin transition. The matrix itself is proportional to the dyadic product of

$$|00\rangle + i|11\rangle \tag{18}$$

with its conjugate, which is clearly nonfactorizable. More generally, entangled pseudo-spinors appear to be associated with the multiple quantum coherences of NMR spectroscopy.

In order to simplify the experiments as well as their analysis and validation, the spectra shown below were obtained by performing the experiments on the $\mathbf{I}_z^1$, $\mathbf{I}_z^2$ and $2\mathbf{I}_z^1\mathbf{I}_z^2$ states separately, and adding the corresponding signals on the spectrometer computer. General methods of generating pseudo-pure states in arbitrary spin systems are under development.

4 An XOR gate via NMR

As is well-known, a quantum XOR gate can be implemented by selective inversion at one of the four peaks in the spectrum, just as in the original ENDOR experiment[1]; this is an example of *Pound-Overhauser double resonance*[4]. While this is often possible in NMR spectroscopy, it can also be difficult if the coupling constant is small. We have therefore developed the following pulse sequence, which constitutes an example of *spin-coherence double resonance*[4], and was easier to use for our initial experiments:

$$\begin{array}{l} [XOR]^2 \equiv [\pi/2]_y^2 - [1/(2J)] - [\pi/2]_x^2 \quad \longleftrightarrow \\ \mathbf{U}_{XOR}^2 = \frac{1}{\sqrt{2}} \begin{pmatrix} 1+i & 0 & 0 & 0 \\ 0 & 1-i & 0 & 0 \\ 0 & 0 & 0 & 1+i \\ 0 & 0 & -1+i & 0 \end{pmatrix} \end{array} \tag{19}$$

The unitary matrix $\mathbf{U}_{XOR}^2$ has the same pattern of zero and nonzero elements as the usual quantum XOR gate (with its output in the second bit), but with phases giving a determinant of 1 instead of -1 as in Pound-Overhauser implementation. We shall call this the *XOR pulse sequence*.

The effect of the XOR pulse sequence on $|10\rangle\langle 10|$, of course, is to convert it to $|11\rangle\langle 11|$. In order to demonstrate this experimentally, however, we must apply further pulses

*In the following, we do not include the effect of the Zeeman Hamiltonian on the density matrix during the delay; equivalently, we implicitly assume that we have placed a π x-pulse in the middle of the $1/(2J)$ period, which refocuses the magnetization at the end of the period.

Product Operator	Initial Spectra		Final Spectra		Product Operator
	$[\pi/2]_y^1$	$[\pi/2]_y^2$	$[\pi/2]_y^1$	$[\pi/2]_y^2$	
$\mathbf{I}_z^1$					$\mathbf{I}_z^1$
$\mathbf{I}_z^2$					$2\mathbf{I}_z^1\mathbf{I}_z^2$
$2\mathbf{I}_z^1\mathbf{I}_z^2$					$\mathbf{I}_z^2$

Table 1: Table of "stick" spectra that would be observed for each of the three diagonal product operators after selective $[\pi/2]_y^k$ observation pulses on the k-th spin, before (initial) and after (final) an XOR pulse sequence (see text).

to convert the unobservable diagonal elements into single quantum coherences. To this end, it is useful to evaluate the action of the XOR sequence on the diagonal product operators, as follows:

$$\begin{aligned}
&\mathbf{I}_z^1 \xrightarrow{[\pi/2]_y^2} \mathbf{I}_z^1 \xrightarrow{[1/(2J)]} \mathbf{I}_z^1 \xrightarrow{[\pi/2]_x^2} \mathbf{I}_z^1 \\
&\mathbf{I}_z^2 \xrightarrow{[\pi/2]_y^2} \mathbf{I}_x^2 \xrightarrow{[1/(2J)]} 2\mathbf{I}_z^1\mathbf{I}_y^2 \xrightarrow{[\pi/2]_x^2} 2\mathbf{I}_z^1\mathbf{I}_z^2 \\
&2\mathbf{I}_z^1\mathbf{I}_z^2 \xrightarrow{[\pi/2]_y^2} 2\mathbf{I}_z^1\mathbf{I}_x^2 \xrightarrow{[1/(2J)]} \mathbf{I}_y^2 \xrightarrow{[\pi/2]_x^2} \mathbf{I}_z^2
\end{aligned} \tag{20}$$

The density matrices of the basic pseudo-pure states given in Eq. (14) are all sums of these three product operators, and thus the spectra that are observed after any pulse sequence is applied to a basic pseudo-pure state are sums of the spectra that would be observed if the same pulse sequence were applied to each of the states $\mathbf{I}_z^1$, $\mathbf{I}_z^2$ and $2\mathbf{I}_z^1\mathbf{I}_z^2$ separately. These spectra are depicted as "stick figures" in Table 1, in which we have separately excited spins 1 and 2 to obtain a complete "readout".

The sum of the inverted initial spectra in the first column therefore shows what we would see after applying a selective $[\pi/2]_y^1$ pulse to the state $|10\rangle\langle 10| \leftrightarrow -\mathbf{I}_z^1 + \mathbf{I}_z^2 - 2\mathbf{I}_z^1\mathbf{I}_z^2$, and consists of a single negative peak with the same total intensity as the positive peak that would be observed after applying a $[\pi/2]_y^2$ pulse. The result of the XOR sequence $|11\rangle\langle 11| \leftrightarrow -\mathbf{I}_z^1 - \mathbf{I}_z^2 + 2\mathbf{I}_z^1\mathbf{I}_z^2$ behaves similarly under the readout pulses, except that the peak observed after a $[\pi/2]_y^1$ pulse is now in phase with the peak obtained after a $[\pi/2]_y^2$ pulse, *and* shifted to the left by the coupling constant J (see Fig. 2).

As a final check, we have also applied the XOR pulse sequence to the superposition $\mathbf{I}_x^1 + \mathbf{I}_x^2 + 2\mathbf{I}_x^1\mathbf{I}_x^2$ that is obtained after applying a nonselective $\pi/2$ y-pulse to the basic pseudo-pure state $\mathbf{I}_z^1 + \mathbf{I}_z^2 + 2\mathbf{I}_z^1\mathbf{I}_z^2$. The superposition gives four lines of equal intensity and phase, just as in Fig. 1. The result of applying the XOR sequence to it is shown in Fig. 3, and consists of four lines of equal intensity as before, but shifted in phase by $\pm\pi/2$ to give four *dispersive* peaks. Thus, our XOR pulse sequence changes the spectrum only by phase factors. The effect on the actual state is to give the superposition obtained by applying a nonselective $\pi/2$ x-pulse to the state $|01\rangle\langle 01| \leftrightarrow \mathbf{I}_z^1 - \mathbf{I}_z^2 - 2\mathbf{I}_z^1\mathbf{I}_z^2$.

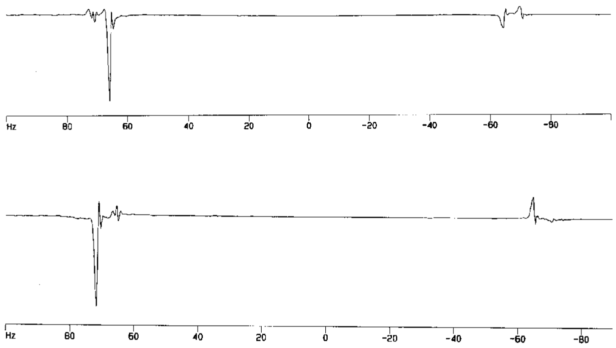

Figure 2: Two experimental NMR spectra of 2,3-dibromothiophene, which illustrate the effect of applying an XOR to the pseudo-pure state $-\mathbf{I}_z^1 + \mathbf{I}_z^2 - 2\mathbf{I}_z^1\mathbf{I}_z^2$ (above) to get $-\mathbf{I}_z^1 - \mathbf{I}_z^2 + 2\mathbf{I}_z^1\mathbf{I}_z^2$ (below). The change in state is indicated by the shift in the position of the peak that is observed following a selective $\pi/2$ y-pulse applied to the first spin.

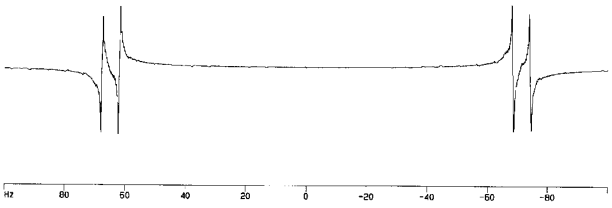

Figure 3: The result of applying the XOR pulse sequence to the superposition $\mathbf{I}_x^1 + \mathbf{I}_x^2 + 2\mathbf{I}_x^1\mathbf{I}_x^2$ is $-\mathbf{I}_y^1 + \mathbf{I}_y^2 - 2\mathbf{I}_y^1\mathbf{I}_y^2$, which is identical to the superposition obtained by applying a $\pi/2$ x-pulse to the basic pseudo-pure state $\mathbf{I}_z^1 - \mathbf{I}_z^2 - 2\mathbf{I}_z^1\mathbf{I}_z^2$.

5 The Toffoli gate

We have also developed a pulse sequence, analogous to the above XOR sequence, which transforms the basic pseudo-spinors of a three-spin system according to the truth table of the well-known Toffoli gate[9]. We call this the *Toffoli pulse sequence*:

$$\begin{aligned}
[TOF]^3 \equiv\ & [\pi/2]_y^3 - [1/(4J)] - [\pi/2]_y^3 - [1/(4J)] \\
& - [-\pi/2]_x^3 - [1/(4J)] - [-\pi/2]_x^3
\end{aligned} \tag{21}$$

Although this pulse sequence assumes that the coupling constants J_{13} and J_{23} have the same value J, it can modified to work with unequal coupling constants as well. Since the Toffoli gate is universal, the existence of this sequence implies that any *special* unitary transformation of pseudo-spinors can be implemented via NMR pulse sequences selective for single spins. Other unitary transformations require the use of pulses that are selective for the individual components in the multiplet of a single spin, as in Pound-Overhauser double resonance.

The matrix of the above Toffoli pulse sequence is easily shown to be $\frac{-1}{\sqrt{2}}$ times:

$$\begin{pmatrix} 1+i & 0 & 0 & 0 & 0 & 0 & 0 & 0 \\ 0 & 1-i & 0 & 0 & 0 & 0 & 0 & 0 \\ 0 & 0 & i & 0 & 0 & 0 & 0 & 0 \\ 0 & 0 & 0 & -i & 0 & 0 & 0 & 0 \\ 0 & 0 & 0 & 0 & i & 0 & 0 & 0 \\ 0 & 0 & 0 & 0 & 0 & -i & 0 & 0 \\ 0 & 0 & 0 & 0 & 0 & 0 & 0 & 1-i \\ 0 & 0 & 0 & 0 & 0 & 0 & -1-i & 0 \end{pmatrix} \tag{22}$$

Hence the output of the gate is in the third bit; the output could easily have been placed in the first or second bit by applying the $\pi/2$ pulses to the corresponding spin.

Once again, the effect of the Toffoli sequence on the actual NMR spectra (after one-spin "readout" pulses) of the eight basic pseudo-pure states is most easily established by determining how it affects the seven diagonal product operators (see Table 2). Unlike the XOR sequence, however, the Toffoli sequence does not simply permute these product operators; instead, it results in a sum of such diagonal operators, e.g.

$$\begin{aligned} \mathbf{I}_z^3 &\xrightarrow{[\pi/2]_y^3} \mathbf{I}_x^3 \\ &\xrightarrow{[1/(4J)]} \tfrac{1}{2}\mathbf{I}_x^3 + \mathbf{I}_z^1\mathbf{I}_y^3 + \mathbf{I}_z^2\mathbf{I}_y^3 - 2\mathbf{I}_z^1\mathbf{I}_z^2\mathbf{I}_x^3 \\ &\xrightarrow{[\pi/2]_y^3} \tfrac{-1}{2}\mathbf{I}_z^3 + \mathbf{I}_z^1\mathbf{I}_y^3 + \mathbf{I}_z^2\mathbf{I}_y^3 + 2\mathbf{I}_z^1\mathbf{I}_z^2\mathbf{I}_z^3 \\ &\xrightarrow{[1/(4J)]} \tfrac{-1}{2}\mathbf{I}_z^3 - \tfrac{1}{2}\mathbf{I}_x^3 + 2\mathbf{I}_z^1\mathbf{I}_z^2\mathbf{I}_x^3 + 2\mathbf{I}_z^1\mathbf{I}_z^2\mathbf{I}_z^3 \\ &\xrightarrow{[-\pi/2]_x^3} \tfrac{-1}{2}\mathbf{I}_y^3 - \tfrac{1}{2}\mathbf{I}_x^3 + 2\mathbf{I}_z^1\mathbf{I}_z^2\mathbf{I}_x^3 + 2\mathbf{I}_z^1\mathbf{I}_z^2\mathbf{I}_y^3 \\ &\xrightarrow{[1/(4J)]} \tfrac{-1}{2}\mathbf{I}_y^3 - \mathbf{I}_z^1\mathbf{I}_x^3 - \mathbf{I}_z^2\mathbf{I}_y^3 + 2\mathbf{I}_z^1\mathbf{I}_z^2\mathbf{I}_y^3 \\ &\xrightarrow{[-\pi/2]_x^3} \tfrac{1}{2}\mathbf{I}_z^3 + \mathbf{I}_z^1\mathbf{I}_z^3 + \mathbf{I}_z^2\mathbf{I}_z^3 - 2\mathbf{I}_z^1\mathbf{I}_z^2\mathbf{I}_z^3 \ . \end{aligned} \tag{23}$$

Similar calculations lead to the following complete list:

$$\begin{aligned} \mathbf{I}_z^1 &\xrightarrow{[TOF]^3} \mathbf{I}_z^1 \\ \mathbf{I}_z^2 &\xrightarrow{[TOF]^3} \mathbf{I}_z^2 \\ \mathbf{I}_z^3 &\xrightarrow{[TOF]^3} \tfrac{1}{2}\mathbf{I}_z^3 + \mathbf{I}_z^1\mathbf{I}_z^3 + \mathbf{I}_z^2\mathbf{I}_z^3 - 2\mathbf{I}_z^1\mathbf{I}_z^2\mathbf{I}_z^3 \\ 2\mathbf{I}_z^1\mathbf{I}_z^2 &\xrightarrow{[TOF]^3} 2\mathbf{I}_z^1\mathbf{I}_z^2 \\ 2\mathbf{I}_z^1\mathbf{I}_z^3 &\xrightarrow{[TOF]^3} \tfrac{1}{2}\mathbf{I}_z^3 - \mathbf{I}_z^2\mathbf{I}_z^3 + \mathbf{I}_z^1\mathbf{I}_z^3 + 2\mathbf{I}_z^1\mathbf{I}_z^2\mathbf{I}_z^3 \\ 2\mathbf{I}_z^2\mathbf{I}_z^3 &\xrightarrow{[TOF]^3} \tfrac{1}{2}\mathbf{I}_z^3 - \mathbf{I}_z^1\mathbf{I}_z^3 + \mathbf{I}_z^2\mathbf{I}_z^3 + 2\mathbf{I}_z^1\mathbf{I}_z^2\mathbf{I}_z^3 \\ 4\mathbf{I}_z^1\mathbf{I}_z^2\mathbf{I}_z^3 &\xrightarrow{[TOF]^3} \tfrac{-1}{2}\mathbf{I}_z^3 + \mathbf{I}_z^1\mathbf{I}_z^3 + \mathbf{I}_z^2\mathbf{I}_z^3 + 2\mathbf{I}_z^1\mathbf{I}_z^2\mathbf{I}_z^3 \end{aligned} \tag{24}$$

Spinor	$\mathbf{I}_z^1$	$\mathbf{I}_z^2$	$\mathbf{I}_z^3$	$2\mathbf{I}_z^1\mathbf{I}_z^2$	$2\mathbf{I}_z^1\mathbf{I}_z^3$	$2\mathbf{I}_z^2\mathbf{I}_z^3$	$4\mathbf{I}_z^1\mathbf{I}_z^2\mathbf{I}_z^3$
$\|000\rangle$	1	1	1	1	1	1	1
$\|001\rangle$	1	1	−1	1	−1	−1	−1
$\|010\rangle$	1	−1	1	−1	1	−1	−1
$\|011\rangle$	1	−1	−1	−1	−1	1	1
$\|100\rangle$	−1	1	1	−1	−1	1	−1
$\|101\rangle$	−1	1	−1	−1	1	−1	1
$\|110\rangle$	−1	−1	1	1	−1	−1	1
$\|111\rangle$	−1	−1	−1	1	1	1	−1

Table 2: Table of coefficients of the seven diagonal product operators corresponding to each basic pseudo-spinor for a three-spin system.

The spectra that are expected from each of these sums, after appropriate one-spin readout pulses, can be worked out in a straightforward fashion, and the experiments needed to validate this, as well as the usual Pound-Overhauser, implementation of the Toffoli gate are underway.

References

[1] DiVincenzo, David P., "Quantum computation", *Science* **270** (1995), 255–261.

[2] Brassard, Gilles, "A quantum jump in computer science", *Computer Science Today* (J. van Leeuwen ed.), Springer-Verlag (1995), 1–14.

[3] Brassard, Gilles, "New trends in quantum computing", *13th Symp. Theor. Aspects Comput. Sci.* (February 1996); (quant-ph/9602014).

[4] Slichter, Charles P., *Principles of Magnetic Resonance* (3rd. ed.), Springer-Verlag (1990).

[5] Goldman, Maurice, *Quantum Description of High-Resolution NMR in Liquids*, Clarendon Press (1988).

[6] Ernst, Richard R., Geoffrey Bodenhausen, and Alexander Wokaun, *Principles of Nuclear Magnetic Resonance in One and Two Dimensions*, Oxford Univ. Press (1987).

[7] Gershenfeld, Neil, Isaac Chuang, and Seth Lloyd, "Bulk Quantum Computation", in this volume.

[8] Cory, David G., Amr F. Fahmy, and Timothy F. Havel, "Ensemble quantum computing by nuclear magnetic resonance spectroscopy", submitted for publication (available as Harvard University Center for Research in Computing Technology Technical Report TR-10-96 from `ftp:deas-ftp.harvard.edu/techreports/tr.html`).

[9] Toffoli, Tommaso, "Reversible computing", *Automata, Languages and Programming* (J. W. de Bakker and J. van Leeuwen ed.), Springer-Verlag (1980), 632–644.